

MODIS Reflective Solar Bands Uncertainty Analysis

Joseph Esposito^a, Xiaoxiong Xiong^b, Aisheng Wu^a, Junqiang Sun^a, and William Barnes^c

^aScience Systems and Applications, Inc., 10210 Greenbelt Road, Lanham, MD 20706

^bEarth Sciences Directorate, NASA/GSFC, Greenbelt, MD 20771

^cUniversity of Maryland, Baltimore County, Baltimore, MD 21250

A key instrument for the NASA Earth Observing System (EOS) mission, the Moderate Resolution Imaging Spectroradiometer (MODIS), is currently operating on-board the Terra and Aqua spacecrafts. This paper discusses the calibration uncertainty analysis for the MODIS Reflective Solar Bands. Each MODIS, either on the Terra or on the Aqua spacecraft, has 20 reflective solar bands, making observations at three different nadir spatial resolutions: 250m (B1-2), 500m (B3-7), and 1000m (B8-19, and B26). The 250m, 500m, and 1000m bands have 40, 20, and 10 detectors per band, respectively. The reflective solar bands spectral wavelengths are between 0.41 and 2.3 μ m. On-orbit, a solar diffuser is used for the reflective solar bands calibration. For the high gain ocean color bands (B8-16), a retractable attenuation pinhole screen is placed in front of the solar diffuser during each calibration. For the reflective solar bands, the specified uncertainty at the typical scene is 2% in reflectance and 5% in radiance. The uncertainty analysis to be presented in this paper will include the approaches and estimated results for Terra MODIS. Aqua MODIS L1B uncertainty is not reported but is extremely similar to Terra. Emphasis will be on the solar diffuser bi-directional reflectance factor characterization at pre-launch since it is a major contributor to the reflective solar bands uncertainty. Other factors include the Earth view response-versus-scan angle, solar diffuser degradation and attenuation screen effect. For the Terra MODIS instrument, the estimated uncertainties based on the instrument characterization and performance will be compared with the specifications.

1. Introduction

The Moderate Resolution Imaging Spectroradiometer (MODIS) currently operating on-board the Terra and Aqua spacecrafts is a key instrument for the NASA Earth Observing System (EOS) mission^{1,2,3,4}. MODIS covers the spectral range from 0.41 μ m to 14.5 μ m with 36 bands at three spatial resolutions: bands B1-B2 at 250m with 40 detectors, bands B3-B7 at 500m with 20 detectors, and bands B8-B36 at 1km with 10 detectors. The spectral range of MODIS is separated into two distinct groups: the reflective solar bands (visible, near infrared, and short wavelength infrared) and the thermal emissive bands (medium and long wavelength infrared). The emissive bands (TEB) are discussed in an accompanying paper. Table 1 contains key specifications for the reflective solar bands (RSB). The RSB uncertainty specification for a typical scene is 2% in reflectance factor and 5% in radiance.

Each of the RSB bands B13-14 has a low and high gain output. This is accomplished by combining the signal from two banks of ten detectors using time delayed integration (TDI) on each detector pair. The combined detector signals for each band are then amplified using independent low gain and high gain electronic paths. The gain of each detector's electronic path, and in fact for all bands B1-30, can be controlled from the ground station using an 8 bit digital to analog converter (D2A).

The RSBs are calibrated on-orbit using a space grade Spectralon™ plate with a near Lambertian reflectance profile as a solar diffuser (SD). A retractable attenuation screen with a transmittance of 8.56% is used during calibration of the high gain ocean color bands, B8-16, to prevent response saturation. Pre-launch calibration of the SD bidirectional reflectance factor (BRF) and instrumental parameters (e.g. thermal changes of detector gain) are combined with on-orbit observations of detector response to calibrate the Level 1B (L1B) deliverable products.

In this report the primary L1B deliverable and the calibration algorithm are briefly reviewed. The uncertainties associated with the L1B algorithm are defined and each is discussed. The total uncertainty for each band is determined and compared with the pre-launch specification. Finally, remaining concerns are addressed.

2. The L1B Reflective Solar Bands Algorithm

The primary deliverable product for the RSBs is the reflectance factor^{5,6}

$$\rho_{EV} \cos(\theta_{EV}) = m_1 dn_{EV}^* d_{E-S}^2, \quad (2.1)$$

where ρ_{EV} is the Earth scene bi-directional reflectance factor (BRF), θ_{EV} is the solar illumination angle of the Earth scene, dn_{EV}^* is the earth scene digital response corrected for instrumental effects, d_{E-S} is the Earth-sun distance at the time of the measurement in units of AU, and m_1 is a calibration scaling factor determined on-orbit using the on-board solar diffuser.

The EV scene digital response, with instrumental parameter correction, for a single band (B), detector (D), frame (F), subframe (S), and scan (N) when mirror side is the index, has the form

$$dn_{EV}^*(B, D, F, S, N) = \frac{dn(B, D, F, S, N)(1 + k_{Inst}(B, D, S, M(N))\Delta T_{Inst, EV})}{RVS(B, D, F, S)}, \quad (2.2)$$

where $M(N)$ is mirror side of the Nth scan, The parameter dn is the scene digital response after correction for dark scene response (the space view (SV) scene average over 50 frames)

$$dn_{EV}(B, D, F, S, N) = DN_{EV}(B, D, F, S, N) - \langle DN_{SV}(B, D, S, N) \rangle. \quad (2.3)$$

DN_{EV} is the raw digital response of the EV scene, $\langle DN_{SV} \rangle$ is the frame averaged dark response offset determined from viewing cold space through the space view port. The coefficient k_{Inst} is the rate of gain-change due to temperature, $M(N)$ is the paddle wheel mirror side for the scan, $\Delta T_{Inst, EV}$ is the temperature difference relative to the nominal pre-launch calibration temperature,

$$\Delta T_{Inst, EV} = T_{Inst, EV} - T_{Inst, Ref}, \quad (2.4)$$

and RVS is the scene response versus scan angle. The RVS is normalized to unity at the angle-of-incidence (AOI) midpoint of the SD, which is 50.25°. Equation (2.2) gives the corrected

single pixel response of an EV scene (equation (2.3) is the uncorrected, measured response for the pixel).

Table 1. Key reflective solar band specifications. The on-orbit SNR is also given for comparison. Note that the SNR specification, in itself, almost yields the 2% reflectance factor specification. The specification is 5% at typical radiance.

Band	Center Wavelength [nm]	Typical Earth scene Radiance L_{Typ} [$W\cdot m^{-2}\cdot sr^{-1}\cdot \mu m^{-1}$]	SNR Specification at L_{Typ}	SNR On-Orbit at L_{Typ}
1	645	21.8	128	186
2	858	24.7	201	517
3	469	35.3	243	328
4	555	29.0	228	330
5	1240	5.4	74	161
6	1640	7.3	275	472
7	2130	1.0	110	147
8	412	44.9	880	1097
9	443	41.9	838	1495
10	488	32.1	802	1521
11	531	27.9	754	1604
12	551	21.0	750	1452
13	667	9.5	910	1413
14	678	8.7	1087	1518
15	748	10.2	586	1519
16	869	6.2	516	1400
17	905	10.0	167	379
18	936	3.6	57	76
19	940	15.0	250	509
26	1375	6.0	150	230

The scaling factor is determined from solar illumination of the solar diffuser

$$m_1 = \left\langle \frac{\rho_{SD} \cos(\theta_{SD})}{\langle dn_{SD}^* \rangle d_{E-S,SD}^2} \Gamma_{SD} \Delta_{SD} \right\rangle \quad (2.5)$$

where equation (2.1) has been used with SD replacing EV, ρ_{SD} is the pre-launch calibrated BRDF of the solar diffuser, $\cos(\theta_{SD})$ is the aspect cosine of solar illumination incident to the SD. The additional on-orbit instrumental parameters Γ_{SD} and Δ_{SD} are the solar diffuser screen (SDS) vignetting and solar diffuser degradation terms respectively. The average of the response, $\langle dn_{SD}^* \rangle$ is over SD sector frames (50) for each scan, with outlier rejection, and the average of the right-hand-side (rhs) is over a selected set of scans (the sweet spot range) for each scan mirror side. The calibration scaling factor m_1 is inherently dependent upon time. Upon

combining equations (2.1) through (2.5) we arrive at the form of the reflectance factor written with all terms shown

$$\rho_{EV} \cos(\theta_{EV}) = \left\langle \frac{\rho_{SD} \cos(\theta_{SD})}{\langle dn_{SD} \rangle} \Gamma_{SD} \Delta_{SD} \right\rangle dn_{EV} \frac{(1+k_{inst} \Delta T_{inst,EV}) d_{E-S,EV}^2 RVS_{SD}}{(1+k_{inst} \Delta T_{inst,SD}) d_{E-S,SD}^2 RVS_{EV}} \quad (2.6)$$

3. The RSB Reflectance Factor Uncertainty

The total uncertainty of the reflectance factor can be written as the rms summation of the uncertainty associated with the parameters on the rhs of equation (2.6)

$$\begin{aligned} \left[\frac{\delta(\rho_{EV} \cos(\theta_{EV}))}{\rho_{EV} \cos(\theta_{EV})} \right]^2 &= \left[\frac{\delta \rho_{SD}}{\rho_{SD}} \right]^2 + \left[\frac{\delta \Gamma_{SD}}{\Gamma_{SD}} \right]^2 + \left[\frac{\delta \Delta_{SD}}{\Delta_{SD}} \right]^2 + \left[\frac{\delta dn_{SD}}{dn_{SD}} \right]^2 + \left[\frac{\delta dn_{EV}}{dn_{EV}} \right]^2 + \\ &\left[\frac{\delta RVS_{EV}}{RVS_{EV}} \right]^2 + \left[\delta k_{inst} (T_{inst,EV} - T_{inst,SD}) \right]^2 + \left[\sqrt{2} \delta((T_{inst,EV} - T_{inst,SD})) k_{inst} \right]^2 \end{aligned} \quad (3.1)$$

where the terms related to temperature correction are related to both dn_{EV}^* and dn_{SD}^* ,

$$\frac{(1 + k_{inst} (T_{inst,EV} - T_{inst,Ref.}))}{(1 + k_{inst} (T_{inst,SD} - T_{inst,Ref.}))} \approx 1 + k_{inst} (T_{inst,EV} - T_{inst,SD}), \quad (3.2)$$

the terms related to solar distance and $\cos(\theta_{SD})$ are dropped since their contributions to the uncertainty are negligible, and the term related to RVS_{SD} is dropped too since the RVS is always normalized at AOI of the SD.

4. The Solar Diffuser BRF Uncertainty

The solar diffuser BRF was calibrated pre-launch at the Santa Barbara Remote Sensing facility in Santa Barbara, CA, in 1997. A comparing goniometer was used for the calibration where the reference sample was calibrated by the National Institute of Standards and Technology (NIST). The calibration incident illumination angles were chosen to cover the anticipated range of Earth-sun on-orbit incident angles and consisted of nine incident vectors on a 3-by-3 grid (see table 3). The dominant term in the L1B reflectance factor uncertainty at typical radiance, L_{Typ} , is the pre-launch measured BRF uncertainty. The total uncertainty arises from measurement uncertainty, both at NIST and at SBRS, uncertainty in the SBRS characterization of the SD BRF, uncertainty in the transfer of the NIST standard at SBRS, spatial non-uniformity of the SD spectralon plate, and uncertainty pre-launch to on-orbit SD BRF change (degradation) uncertainty. Values associated with the SD BRF uncertainty for Terra and Aqua MODIS are given in Table 4^{7,8}. The values in Table 4 are independent uncertainties and the root-squared-sum technique is appropriate for computing the total BRF uncertainty. Two of the component values, spectral interpolation and stray light, are not part of the BRF calibration. The value of each of these

terms is conservative pre-launch estimates. The BRF uncertainty contribution is the dominant term in the L1B reflectance factor uncertainty.

5. The Solar Diffuser Screen Vignetting Function Uncertainty

The SDS vignetting function was intended to only affect the high gain bands (bands 8-16) which are primarily used by the Oceans Science Team. On mission day 2003126 the Terra SDS failed to open. It was decided to set the solar diffuser door (SDD) to open position starting on mission day 2003183 and leave the SDS in closed position. Due to this the SDS vignetting function uncertainty affects all RSBs on and after mission day 2003183. This increases the Terra uncertainty slightly for the non-ocean RSBs, B1-B7, B17-B19, and B26, after mission day 2003183.0.

The vignetting function of both Terra and Aqua have been characterized on-orbit for bands B1-4 and B17-19 during spacecraft yaw maneuvers as polynomial surfaces. The average of these results for bands 17-19 is used, detector by detector, to produce vignetting functions for the high gain ocean color bands. For Terra, an additional vignetting function has been produced through trending analysis of the measured m_1 for bands B1-4 and B17-19 and fitting as a time dependent function of the spacecraft beta angle, the angle between the spacecraft orbital plane and the sun. This empirical vignetting function (EVF) is applied in addition to the vignetting function fitted in the yaw characterization. Trending of the measured m_1 results over the mission yields 0.5% as the upper bound for the total SDS vignetting function uncertainty.

Table 3. The incident angle grid, in the instrument coordinate system, that was used during the pre-launch SD calibration [degrees].

Instrument Declination/Azimuth		
10.0/-13.0	10.0/-23.0	10.0/-33.0
13.5/-13.0	13.5/-23.0	13.5/-33.0
17.0/-13.0	17.0/-23.0	17.0/-33.0

Table 4. The pre-launch characterization uncertainties of the solar diffuser BRF^{7,8} [%]. This value is used for all bands (wavelengths). A stray light term is included.

NIST Reference	0.50
SBRs Characterization	0.70
NIST Transfer to MODIS	0.50
SD $\sigma_{Spatial}$	0.70
Pre-launch to on-orbit	0.50
SD BRF Characterization	0.50
Spectral Interpolation	0.10
Stray Light	0.30
Total BRF Uncertainty (RSS)	1.44

6. The Solar Diffuser Degradation Function Uncertainty

The SD degradation function is measured on-orbit using the Solar Diffuser Stability Monitor (SDSM). The SDSM contains nine detectors, placed within a small Spectral Integrating Sphere (SIS), that are associated with the spectral response of nine MODIS bands. The MODIS band to SDSM detector association is given in table 5. In each calibration, the SDSM operates as a ratioing radiometer, comparing the detector response of the SDSM viewing the solar diffuser to

the detector response of the SDSM viewing the attenuated solar irradiance. The incident light path within the SDSM is identical for both views. The comparison removes response changes due to detector variability, solar distance, and degradation of the SDSM SIS.

The pinhole attenuation screen is the cause of ~10% ripples in the SDSM solar view response. In order to reduce the response variation due to rippling, the SDSM SD view and solar view for each detector is normalized, sample-by-sample, with the respective response of SDSM detector 9 (936 nm). Laboratory VUV results indicate that the degradation of space grade spectralon is negligible at and above this wavelength. Therefore, the ratio of the averaged normalized response is used to determine the SD degradation.

Trended ratio data from each detector in the SDSM is fitted with an exponential function of the form

$$f(t) = Ae^{-\alpha(t-t_0)} \tag{6.1}$$

where the normalization time t_0 is chosen to be near the time of the NADIR door opening. The SD degradation is obtained from the SDSM data

$$\Delta(t) = e^{-\alpha(t-t_0)} \tag{6.2}$$

Table 5. The center wavelength and bandwidth of the filtered Terra SDSM detectors are given. The associated MODIS band, BCWL, and bandwidth are also tabulated. The closeness of the center wavelength and bandwidth is due to the Terra SDSM detector filters being from the same batch as Terra MODIS detector filters.

SDSM Detector	SDSM Center Wavelength [nm]	Bandwidth [nm]	MODIS Band	MODIS BCWL [nm]	Bandwidth [nm]
1	411.97	11.46	8	411.80	11.80
2	465.69	17.26	3	465.60	17.60
3	529.74	11.68	11	529.70	11.80
4	553.75	19.70	4	553.70	19.70
5	646.14	42.50	1	646.50	41.80
6	746.62	9.98	15	746.40	10.00
7	856.49	39.28	2	856.70	39.40
8	904.29	35.81	17	904.10	35.70
9	936.23	45.80	19	936.10	46.30

The uncertainty of $\Delta(t)$ is determined from the RMS difference of the fitted line to the data. The RMS result is bounded by a maximum and minimum uncertainty, 0.5% (detector 1 at 412nm) and 0.2% (at and above 936nm) respectively.

Early in the Terra MODIS and Aqua MODIS missions, RSB calibrations (along with the SDSM calibrations) were performed weekly, with one orbit for open SDS and one orbit for the closed SDS calibration. The calibration rate was later reduced to bi-weekly calibrations. The Aqua

MODIS currently remains on this bi-weekly schedule, with two orbits, one SDS open and one SDS closed, per calibration. Terra MODIS followed the bi-weekly schedule with two orbits per calibration until May 6 2003, when the SD screen failed to open and no further attempts were made to open it because of the risk of further failures. Thus, from July 2, 2003 onward the SD door would remain open but the SD screen would remain closed indefinitely. This configuration has allowed for a RSB calibration to be performed every orbit, which has been done. For delivered calibration coefficients, the new calibration schedule for Terra remains bi-weekly, but it now averages one day's worth of orbits (14-15 orbits) to perform the SDS closed calibration instead of only one orbit. There is no SDS open calibration for Terra because the SD screen is not opened.

7. The Response Uncertainty

The fractional uncertainty associated with the solar diffuser calibration response is equal to the inverse of the signal to noise ratio (SNR) during a typical calibration for an SD response within the calibration sweet spot. The response and uncertainty is calculated for each scan and a linear uncertainty vs. response function is then fitted with the data. The SNR is calculated using the fitted function at the typical response corresponding to the typical Earth view scene radiance, L_{Typ} . The fractional uncertainty associated with SD responses is derived from the SD calibration data. The fractional SD response uncertainty, $\sigma_{dn}(dn_{SD})/dn_{SD}$, and EV scene response uncertainty, $\sigma_{dn}(dn_{EV})/dn_{EV}$, is tabulated below (table 6).

8. The Earth Scene RVS Uncertainty

The Earth scene RVS uncertainty has been determined from the pre-launch calibration. The RVS was measured at SBRS for each [B,D,M] at selected AOIs evenly distributed in the region of the EV sector' AOI from 10.5° to 65° using the Spherical Integrating Source 100 (SIS100). The SIS100 response data was averaged over scans for each of the AOIs. The response data was fitted to a quadratic form and the quadratic form was then normalized at the SD angle of incidence (AOI), 50.25°, for each [B,D,M]. There is no RVS subframe dependence because this is a negligible effect.

It has been determined on-orbit that the RVS of MODIS is time and AOI dependent. Additionally, the ratio of Terra relative mirror side RVS degradation is not unity. On-orbit spectroradiometric calibration assembly (SRCA) measurements and lunar observations through the SV port, at AOI 38.0° and 11.4° respectively, are used to trend the time and AOI dependence of the RVS. Additional RVS uncertainty due to the time and AOI is taken at an upper limit of 0.5%. The RVS uncertainty characterized pre-launch and this additional on-orbit characterized uncertainty are given separately in table 6.

9. The Temperature Correction Uncertainty

The gain of the MODIS detectors is affected by the ambient temperature of the focal plane arrays (FPAs) and the instrument electronics. During pre-launch thermal-vacuum chamber calibration the uncooled FPAs and instrument electronics were thermally saturated to the same temperature

at each thermal plateau and the effect upon the detector gain could not be separated. Therefore, the temperature correction consists of a single linear coefficient, k_{Inst}

$$\text{Corr}(T_{\text{Inst}}) = 1 + k_{\text{Inst}} \Delta T_{\text{Inst}}; \Delta T_{\text{Inst}} = T_{\text{Inst}} - T_{\text{Inst-Ref.}} \quad (9.1)$$

where $T_{\text{Inst,Ref}}$ is the chosen reference temperature for Terra and Aqua respectively during pre-launch calibration. The temperature correction is applied to both the dn_{SD} and dn_{EV} responses and enters eq. (3.1) as

$$\rho_{\text{EV}} \cos(\theta_{\text{EV}}) \propto \frac{(1 + k_{\text{Inst}} \Delta T_{\text{Inst,EV}})}{(1 + k_{\text{Inst}} \Delta T_{\text{Inst,SD}})} \approx 1 + k_{\text{Inst}} (T_{\text{Inst,EV}} - T_{\text{Inst,SD}}) \quad (9.2)$$

The uncertainty associated with eq. (9.2) due to error in k_{Inst} has the form

$$\frac{\partial(\rho_{\text{EV}} \cos(\theta_{\text{EV}}))}{\partial k_{\text{Inst}}} \delta k_{\text{Inst}} \leq (T_{\text{Inst,EV}} - T_{\text{Inst,SD}}) \delta k_{\text{Inst}} \quad (9.3)$$

to first order in $(T_{\text{Inst,EV}} - T_{\text{Inst,SD}}) k_{\text{Inst}}$. The value of $(T_{\text{Inst,EV}} - T_{\text{Inst,SD}}) \delta k_{\text{Inst}}$ is typically less than 10^{-3} .

The uncertainty associated with eq. (9.2) due to the error in temperature difference, $\delta(T_{\text{Inst,EV}} - T_{\text{Inst,SD}})$, has a similar form to eq. (9.3) and is conservatively given by $\sqrt{2} \delta(T_{\text{Inst,EV}} - T_{\text{Inst,SD}}) k_{\text{Inst}}$. This uncertainty is also typically less than 10^{-3} .

10. The Total RSB L1B Reflectance Factor Uncertainty

The total L1B band center detector reflectance factor uncertainty for the RSB bands at typical radiance is summarized in table 6 for Terra. The table includes values for each of the terms described above. Terms that have not been included are either unknown or are small and contribute negligibly to the root-square-sum (RSS). All bands, except for band 18 for which the SNR specification is too low to achieve the uncertainty specification, are within the specification of 2% in Earth scene reflectance factor uncertainty which leads to being within the specification of 5% in Earth scene radiance. This analysis does not include bad detectors. Worst case is taken when appropriate and the RSS values in table 6 are an estimate of the upper bound for the reflectance factor uncertainty. Figure 1 depicts contributions to the L1B fractional reflectance factor uncertainty at L_{Typ} as a function of band for Terra. All bands are within the specification for a typical radiance level except band 18, having the lowest response at typical radiance, is slightly above the 2% limit at L_{Typ} . The results for Aqua are comparable to those given for Terra with the caveats: (i) Aqua band 6 has several dead detectors which affect the resulting images at 1640nm; (ii) The SWIR cross-talk is worse for Terra than for Aqua due to pre-launch lessons learned. An electronic cross talk correction has not been applied in the L1B product due to the large amount of computing time that is needed. This results in a slightly higher uncertainty for the Terra SWIR bands and a negligible increase in the Aqua SWIR bands.

11. Summary

There are many contributions to the total RSB reflectance factor uncertainty. The dominant contribution at typical observed radiance (L_{Typ}) is due to the measurement uncertainty in the solar diffuser BRF. Smaller contributions from other sources were also considered. The pre-launch L1B RSB specified uncertainty is 2% in reflectance factor and 5% in radiance.

The equations for determining the uncertainty of the L1B RSB reflectance factor deliverable is derived. Each contribution is discussed and calculated. Contributions to the uncertainty due to solar distance and solar zenith angle are negligible and have been dropped. The total uncertainty in the L1B reflectance factor is given, which reflects the current best estimate. The RSS for all bands, with the exception of band 18, is within the specification at L_{Typ} . The L1B reflectance factor uncertainty for Aqua is comparable to that given for Terra.

References

1. W. L. Barnes, T. S. Pagano, and V. Salomonson, "Prelaunch Characteristics of the Moderate Resolution Imaging Spectroradiometer (MODIS) on EOS-AM1", *IEEE Trans. Geosci. Remote Sensing*, v. 36, pp 1088-1100, 1988.
2. B. Guenther, G. D. Godden, X. Xiong, E. J. Knight, S. Y. Qiu, H. Montgomery, M. M. Hopkins, M. G. Khayat, and Z. Hao, "Prelaunch algorithm and data format for the level 1 calibration products for the EOS-AM1 moderate resolution image spectroradiometer (MODIS)", *IEEE Trans, Geosci. Remote Sensing* 36, pp 1142-1151, 1998.
3. X. Xiong, K. Chiang, J. Esposito, B. Guenther, and W. Barnes, MODIS on-orbit calibration and characterization, *Metrologia*, 2002.
4. X. Xiong, J. Sun, J. Esposito, B. Guenther, and W. Barnes, "MODIS Reflective Solar Bands Calibration Algorithm and On-orbit Performance", *Proceedings of SPIE – Optical Remote Sensing of the Atmosphere and Clouds III*, 2002.
5. X. Xiong, A. Wu, J. Esposito, J. Sun, and N. Che, "Trending Results of MODIS Optics On-Orbit Degradation", *SPIE -Earth Observing Systems VIII*, pp 337-346, 2002.
6. B. Guenther, X. Xiong, V. V. Salomonson, W. L. Barnes, and J. Young, "On-Orbit performance of the Earth Observing System Moderate Resolution Imaging Spectroradiometer; first year of data", *Remote Sensing of the Environment*, v 83, pp 16-30, 2002.
7. J. B. Young, "Summary of PFM solar diffuser BRF characterization and associated reflectance uncertainties," *Internal Report, SBRS*, PL3095-N06370A, 1998
8. J. B. Young, "Summary of FM1 solar diffuser BRF characterization and associated reflectance uncertainties," *Internal Report, SBRS*, PL3095-N07132A, 1999

Table 6. The fractional uncertainties of the terms contributing to the Terra Earth scene reflectance factor at typical radiance (L_{Typ}) are summarized. The uncertainty values are given in percent. The last column contains the total reflectance factor uncertainty. The small response value at L_{Typ} is the cause of the large RSS value for band 18. The RSS is a conservative estimate of the LIB uncertainty.

Band	BRF Error	NEdn _{SD} at L _{SD}	T _{Inst} Error	K _{Inst} Error	SWIR OOB Error	SD Degradation Error	SDS Error	Pre-launch RVS Error At NADIR	On-orbit RVS Error	NEdn _{EV} at L _{Typ}	RSS
1	1.44	0.059	0.010	0.048	0.000	0.370	0.500	0.180	0.500	0.537	1.747
2	1.44	0.050	0.020	0.124	0.000	0.250	0.500	0.014	0.500	0.193	1.646
3	1.44	0.041	0.007	0.130	0.000	0.470	0.500	0.048	0.500	0.305	1.710
4	1.44	0.038	0.008	0.024	0.000	0.420	0.500	0.045	0.500	0.303	1.692
5	1.44	0.086	0.009	0.021	0.100	0.200	0.500	0.033	0.500	0.622	1.742
6	1.44	0.063	0.002	0.040	0.100	0.200	0.500	0.033	0.500	0.212	1.641
7	1.44	0.089	0.006	0.006	0.100	0.200	0.500	0.033	0.500	0.682	1.765
8	1.44	0.212	0.018	0.011	0.000	0.500	0.500	0.045	0.500	0.091	1.702
9	1.44	0.117	0.008	0.094	0.000	0.480	0.500	0.037	0.500	0.067	1.688
10	1.44	0.083	0.006	0.032	0.000	0.460	0.500	0.072	0.500	0.066	1.679
11	1.44	0.092	0.006	0.036	0.000	0.430	0.500	0.062	0.500	0.062	1.671
12	1.44	0.083	0.006	0.011	0.000	0.420	0.500	0.061	0.500	0.069	1.668
13	1.44	0.057	0.008	0.010	0.000	0.350	0.500	0.298	0.500	0.071	1.676
14	1.44	0.042	0.007	0.008	0.000	0.350	0.500	0.281	0.500	0.066	1.673
15	1.44	0.063	0.012	0.015	0.000	0.310	0.500	0.007	0.500	0.066	1.642
16	1.44	0.057	0.009	0.065	0.000	0.240	0.500	0.007	0.500	0.071	1.631
17	1.44	0.020	0.005	0.011	0.000	0.220	0.500	0.030	0.500	0.264	1.646
18	1.44	0.031	0.010	0.052	0.000	0.200	0.500	0.029	0.500	1.309	2.085
19	1.44	0.022	0.003	0.012	0.000	0.200	0.500	0.007	0.500	0.197	1.634
26	1.44	0.044	0.007	0.077	0.100	0.200	0.500	0.033	0.500	0.435	1.685

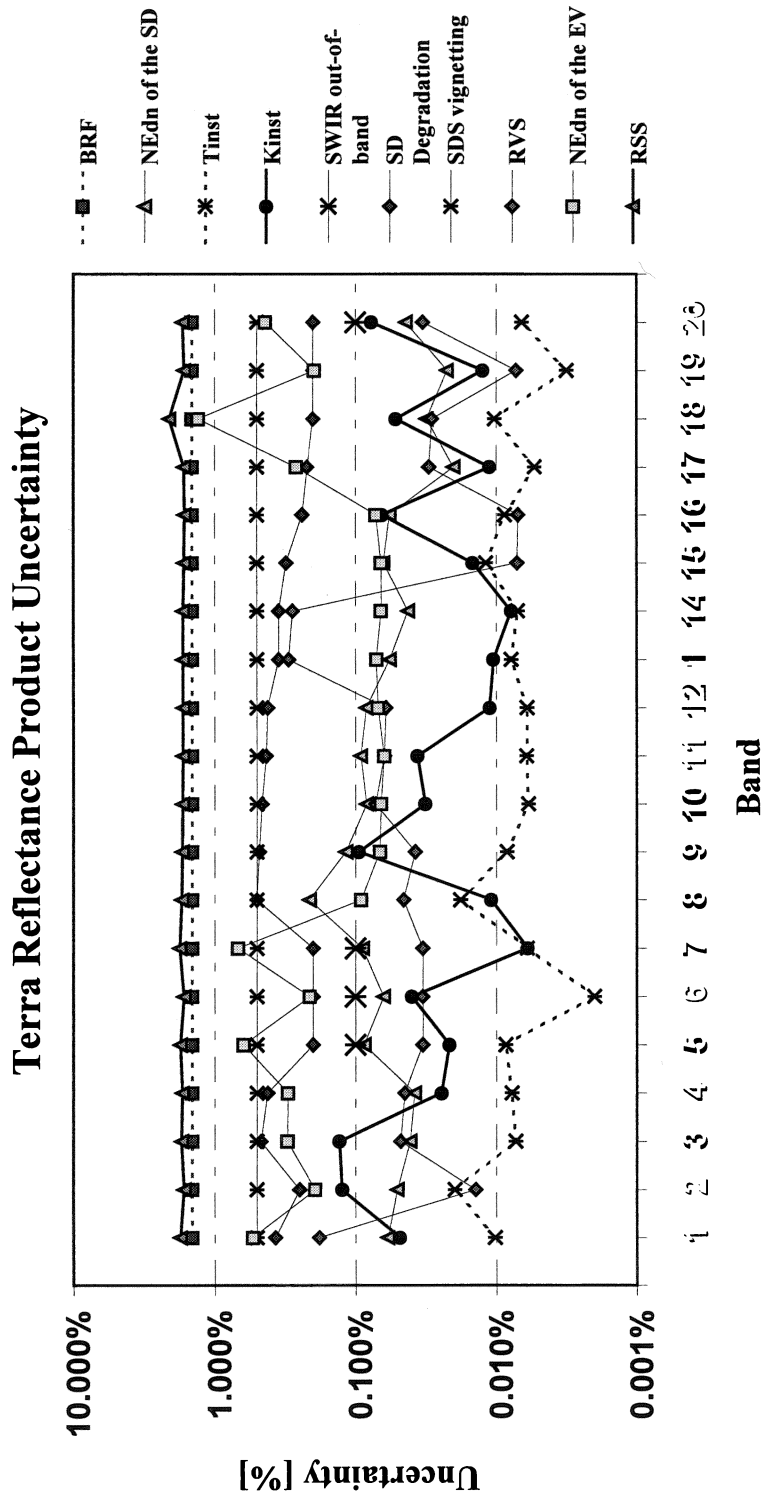


Figure 1. The contributions to the Terra total reflectance factor uncertainty at L_{Typ} for the RSB is shown as a function of band. Note that for L_{Typ} the uncertainty is within the 2 specification for all bands except band 18. Band 18 cannot reach the specification due to the low SNR specification which was required resulting in a lower than necessary response at L_{Typ} .